JACS
JOURNAL OF THE AMERICAN CHEMICAL SOCIETY

Communication

pubs.acs.org/JACS

Exclusive Csp^3–Csp^3 vs Csp^2–Csp^3 Reductive Elimination from Pt^{IV} Governed by Ligand Constraints

Eric G. Bowes,[†] Shrinwantu Pal,[†] and Jennifer A. Love*

Department of Chemistry, The University of British Columbia, Vancouver, British Columbia V6T 1Z1, Canada

Supporting Information

ABSTRACT: Selective reductive elimination of ethane (Csp^3-Csp^3 RE) was observed following bromide abstraction and subsequent thermolysis of a Pt^{IV} complex bearing both Csp^3- and Csp^2-hybridized hydrocarbyl ligands. Through a comparative experimental and theoretical study with two other Pt^{IV} complexes featuring greater conformational flexibility of the ligand scaffold, we show that the rigidity of a meridionally coordinating ligand raises the barrier for Csp^2-Csp^3 RE, resulting in unprecedented reactivity.

Homogeneous selective C-H functionalization of hydrocarbons is one of the grand challenges of organometallic chemistry. Unsaturated Pt^{II} and Pt^{IV} complexes are considered as critical intermediates in both established and proposed processes for methane functionalization,[1] and their intermediacy has been demonstrated in stoichiometric C-H activation and reductive elimination (RE).[2] Building on this knowledge and our own studies of Pt-catalyzed C-X functionalization,[3] we envisioned a possible catalytic system for hydrocarbon functionalization (Scheme 1).

In this proposed catalytic cycle, a neutral Pt^{II} dihydrocarbyl species, **A**, could undergo oxidative addition (OA) of a Csp^2-X bond to form a Pt^{IV} trihydrocarbyl complex, **B**. At present, such a process is only possible by tethering the aryl group to the ligand scaffold.[4] Halide abstraction from **B** would generate cationic, five-coordinate **C**. Based on the work of Goldberg et al.,[5] formation of this species should allow for RE to occur, releasing the functionalized product and an unsaturated Pt^{II} center, **D**. Complexes of type **D** are well-known to activate hydrocarbons, including methane,[1a] through coordination of the C-H bond to the vacant site of the unsaturated Pt^{II} center (complex **E**) followed by OA to form a transient hydrido Pt^{IV} intermediate, **F**. Concomitant deprotonation in the presence of a base[6] would lead to regeneration of **A**. Although the need to tether the aryl halide oxidant (preventing turnover) and the possibility of intramolecular C-H activation of the ligand scaffold represent limitations of this strategy, we sought to establish the feasibility of the process depicted in Scheme 1 through single-step stoichiometric transformations. These studies would provide the proof-of-concept necessary to develop a catalytic system.

Selectivity for Csp^2-Csp^3 RE from **C** is essential to the realization of this process. It is generally observed[7] that the preference for RE follows the order Csp^2-Csp^2 > Csp^2-Csp^3 > Csp^3-Csp^3, a trend that has been corroborated theoretically.[7b,c] Exceptions to this trend have been noted:[8] for Csp^2-Csp^3 vs Csp^3-Csp^3 coupling, Williams et al. reported competitive RE from a Pt^{IV} NCN-pincer complex, albeit still in favor of Csp^2-Csp^3 coupling,[8a] and Puddephatt reported ethane loss from $PtIMe_2(4\text{-}MeC_6H_4)(PMe_2Ph)_2$ in the solid state.[8b] However, selective control of RE from Pt^{IV} centers in solution resulting in well-defined products has, to the best of our knowledge, never been reported. Here we report examples of selective Csp^2-Csp^3 and Csp^3-Csp^3 RE from trihydrocarbyl Pt^{IV} complexes differing in their ligand scaffolds. We demonstrate, through a comparative experimental and theoretical study, that the unexpected selectivity for Csp^3-Csp^3 RE observed is governed by the rigidity and coordination geometry of the Csp^2 group.

We selected **1a** for initial study (Chart 1), prepared by Csp^2-Br activation of $Me_2NCH_2CH_2N{=}CHAr$ (Ar = *o*-BrC_6H_4) by $[PtMe_2(\mu\text{-}SMe_2)]_2$ as previously reported.[9] Removal of bromide from the coordination sphere of reportedly thermally stable[10] **1a** is achieved by treatment with 1 equiv of $AgBF_4$. When performed in CD_3CN, halide abstraction leads to quantitative formation of solvent complex **1b·CD$_3$CN** (Scheme 2), which displays unique ^1H NMR signals for axial and equatorial Pt-CH_3 groups at 0.67 (J_{PtH} = 77.3 Hz) and 0.86 ppm (J_{PtH} = 62.6 Hz).

Scheme 1. Proposed Catalytic Cycle for C-H Functionalization

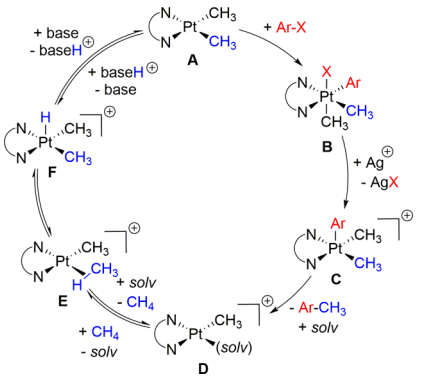

Chart 1. Neutral Pt^{IV} Complexes Investigated in This Study

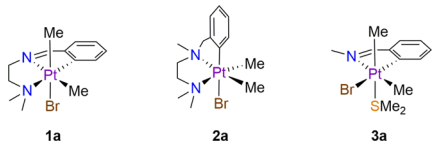

Received: October 20, 2015
Published: December 16, 2015

DOI: 10.1021/jacs.5b10993
J. Am. Chem. Soc. 2015, 137, 16004–16007

Scheme 2. Dehalogenation of 1a

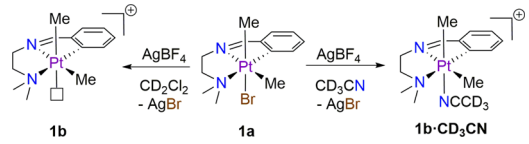

Scheme 3. Csp^3-Csp^3 Reductive Elimination from 1b

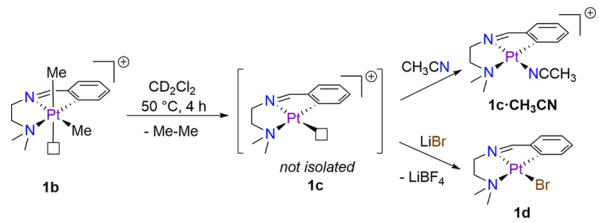

Although **1b·CD_3CN** is stable in CD_3CN solutions, removal of solvent leads to partial decomposition, and attempts to observe **1b·CD_3CN** by means of ESI^+-MS were unsuccessful. ESI^+-MS experiments showed a signal at m/z = 414.1, corresponding to a molecular cation 30 amu lighter than **1b·CD_3CN**. Similar results were obtained when dehalogenation was performed in CH_3CN, giving a signal with m/z = 411.1; we presume that a combination of elevated temperatures and desolvation may be responsible for the loss of ethane (*vide infra*). When dehalogenation is performed in weakly coordinating solvents such as CD_2Cl_2, the five-coordinate complex **1b** is observed. Evidence for the unsaturated nature of **1b** is supported by ^1H NMR data that show the two Pt-Me groups to be equivalent on the NMR time scale at 25 °C, appearing as a singlet at 0.92 ppm with ^{195}Pt satellites (Supporting Information, Figure S1a). Cooling the sample to −48 °C results in the resolution of two unique signals for the axial and equatorial Pt-Me groups at 0.79 (J_{PtH} = 81 Hz) and 0.86 ppm (J_{PtH} = 61 Hz) (Figure S1b). The larger J_{PtH} coupling observed for the axial methyl group can be attributed to the absence of a ligand in the *trans* position. These observations are consistent with exchange of axial and equatorial methyl positions at room temperature,[11] clearly demonstrating that isomerization is faster than reductive coupling in this system.

Upon gentle heating of a CD_2Cl_2 solution of **1b** at 50 °C in a sealed tube, a characteristic singlet corresponding to ethane at 0.86 ppm appeared in the ^1H NMR spectrum. Owing to the insolubility of the resultant Pt^{II} complex **1c** in CD_2Cl_2, the formation of the organometallic product could not be monitored by NMR spectroscopy. The solvated product, **1c·CH_3CN**, was isolated in quantitative yield by removal of CD_2Cl_2 and addition of CH_3CN (Scheme 3). **1c·CH_3CN** has a characteristic HC═N ^1H NMR chemical shift (δ = 8.51 ppm) with large ^{195}Pt coupling (J_{PtH} = 142 Hz), indicative of both reduction to Pt^{II} and the presence of the weak *trans* influencing ligand CH_3CN. The bound CH_3CN group also exhibits ^{195}Pt coupling (J_{PtH} = 12.4 Hz). No signals are present in the Pt-Me or Ar-CH_3 regions, and the *ipso*-C of the Pt-aryl moiety shows ^{195}Pt satellites (J_{PtC} = 101 Hz). Further structural confirmation was provided by conversion to the neutral bromide complex **1d** with LiBr, which has been prepared previously by C-Br activation at Pt^0.[11]

The observation of competitive Csp^2-Csp^3 and Csp^3-Csp^3 RE by Williams et al. involved an aryl ring that was incorporated in a pincer ligand, limiting its mobility.[8a] We hypothesized that the rigid meridional coordination of the C,N,N ligand in **1b** played a role in raising the relative barrier for Csp^2-Csp^3 RE. We therefore

Scheme 4. Synthesis and Molecular Structure of 2a[a]

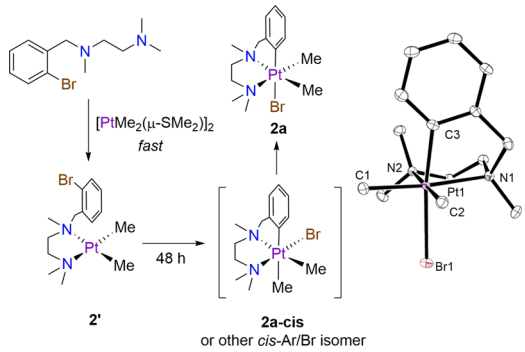

[a]Thermal ellipsoids shown at the 50% probability level.

Scheme 5. Dehalogenation of 2a and Subsequent Csp^2-Csp^3 Reductive Elimination

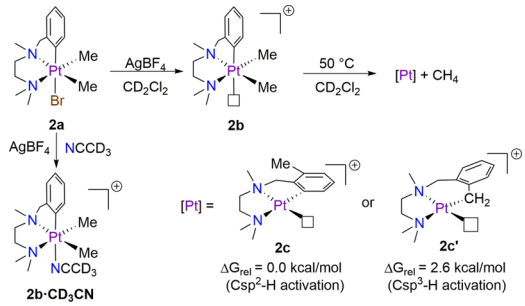

sought to prepare a more flexible complex, **2a**, by C-Br activation of the saturated ligand $Me_2NCH_2CH_2N(Me)CH_2Ar$ (Ar = *o*-BrC_6H_4). κ^2-Ligation to the Pt center is almost instantaneous, forming **2′**.[11] In contrast, C-Br activation was found to be slow. After 48 h, the new Pt^{IV} complex **2a** was formed (Scheme 4), presumably via intermediate **2a-cis**, resulting from concerted OA. X-ray analysis of crystals of **2a** revealed a facial arrangement of the two *N*-donors and aryl fragment about the Pt^{IV} center, in contrast to the *mer* arrangement observed for **1a**.

Dehalogenation of **2a** in CD_3CN similarly yields a solvento complex, **2b·CD_3CN** (Scheme 5). ^1H NMR data indicate that the solvento complex also adopts a *fac*-C,N,N geometry[12] This observation is consistent with DFT calculations that indicate that the *mer* isomer is less stable by 8.2 and 5.1 kcal/mol, for **2a** and **2b**, respectively. As was observed for **1b**, the ^1H NMR spectrum of **2b** in CD_2Cl_2 (Figure S1c) indicates fluxionality at room temperature, by fast exchange of inequivalent Pt-Me groups or by *fac*/*mer* isomerization. Cooling the sample results in the resolution of two Pt-Me signals (Figure S1d). Interestingly, an ESI^+-MS analysis of the CD_3CN solution containing **2b·CD_3CN** revealed a signal at m/z = 416.2 corresponding to **2b**. We presume higher RE barriers from **2b** allow for its observation in ESI^+-MS, consistent with our calculated activation barriers.[12] In addition to the signal for **2b**, a signal with m/z = 400.2 was observed, corresponding to the loss of methane.

Heating a solution of **2b** in CD_2Cl_2 at 50 °C results in slow RE as evidenced by the formation of (δ = 0.21 ppm) and the disappearance of **2b** by ^1H NMR spectroscopy. Notably, under the same experimental conditions used for RE from **1b**, *no ethane was observed*. Formation of methane is consistent with C-H activation of the Csp^2-Csp^3 RE product to form a transient Pt^{IV} hydridodihydrocarbyl complex, followed by Csp^3-H RE. Both Csp^2-H and Csp^3-H activation are possible, resulting in the

DOI: 10.1021/jacs.5b10993
J. Am. Chem. Soc. 2015, 137, 16004−16007

formation of five- (**2c**) and six-membered (**2c′**) metallacycles, respectively (Scheme 5). The ESI$^+$-MS data are consistent with the formation of **2c** or **2c′**.

Unfortunately, we were unable to characterize the Pt^{II} product(s) by NMR spectroscopy. The synthesis of **2a-d_6** (Scheme 6) allowed us to differentiate between the two isomeric products, **2c-d_3** and **2c′-d_2**, by high-resolution mass spectrometry. **2a-d_6** was dehalogenated to form **2b-d_6**, which was then subjected to the same conditions as **2b** was for RE. The formation of **2c′-d_2** (and not **2c-d_3**) was confirmed by ESI$^+$-MS, and CD_4 was observed as the only isotopologue of methane in the ^{2}H NMR spectrum. The competitive formation of six-membered metallacycles via Csp^3-H activation has been noted previously.[10] Our DFT calculations show that the five-membered metallacycle **2c** is the thermodynamic product, suggesting that the final C-H activation step proceeds under kinetic control. It was found computationally that, unlike the arene complexes formed immediately following Csp^2-Csp^3 reductive coupling from **1b** or **3b** (*vide infra*), the product of reductive coupling from **2b** is a σ-(Csp^3-H) complex, presumably due to the preference of the reduced ligand to adopt a folded (*fac*) geometry. The initial formation of a σ-(Csp^3-H) metal interaction may explain the kinetic selectivity observed in this system.

Exclusive Csp^2-Csp^3 RE from **2b** can be understood by considering the pathways available from the lowest energy isomer. Previous work has shown that C-C RE from Pt^{IV} must involve the apical hydrocarbyl group.[5] As such, Csp^3-Csp^3 RE from the *fac* isomer is not possible. Formation of the *mer* isomer (from which there are pathways for both Csp^2-Csp^3 and Csp^3-Csp^3 RE) from **2b** was calculated to be endergonic by 5.1 kcal/mol, leading to a higher activation barrier for Csp^3-Csp^3 RE (32.8 kcal/mol) when compared to the barrier for Csp^2-Csp^3 loss from the *fac*-isomer (27.6 kcal/mol).[12]

Complex **3a**, featuring a bidentate C,N ligand (Chart 1), was prepared using the same methods as for **1a** and **2a**. **3a** exhibits two ^{1}H NMR singlets at 0.98 (J_{PtH} = 71 Hz) and 1.25 ppm (J_{PtH} = 69 Hz) respectively for the axial and equatorial methyl groups. The bound SMe_2 group appears at 2.07 ppm and also exhibits ^{195}Pt coupling (J_{PtH} = 13 Hz). As Pt-Me groups *trans* to Br and SMe_2 groups are expected to exhibit similar ^{195}Pt coupling, a NOESY experiment was performed to aid in assignment of geometry, allowing us to assign **3a** as the isomer with Br *trans* to the aryl group.[12]

Halide abstraction from **3a** in acetonitrile forms a single isomer that slowly loses SMe_2 to give a thermally stable bis-acetonitrile species. Following dehalogenation in acetone-d_6, at least four different species were observed by ^{1}H NMR spectroscopy, all with ^{195}Pt coupling indicative of a Pt^{IV} oxidation state. In CD_2Cl_2, halide abstraction results in the formation of a single broad Pt-Me signal by ^{1}H NMR spectroscopy (Figure S1e), similar to what was observed for **1b**. Cooling this solution to −85 °C results in the resolution of a number of different Pt-Me signals, similar to those observed when dehalogenation was performed in acetone-d_6 (Figure S1f). We propose that unsaturated **3b** and the acetone complex **3b·solv** exist as a mixture of isomers, and possibly form dimers via bridging SMe_2 groups. In acetone-d_6, ^{1}H-^{1}H NOESY data also suggest that disproportionation leads to the formation of a bis-SMe_2 complex.[12] To support this hypothesis, LiBr was added to the mixture of isomers, forming **3a** in quantitative yield (Scheme 7).

Scheme 6. Reductive Elimination from 2b-d_6

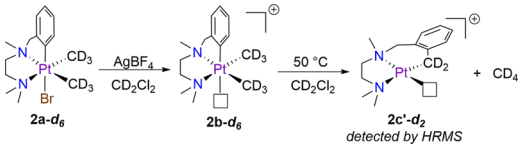

Scheme 7. Reactivity following Dehalogenation of 3a and Molecular Structure of 3d[a]

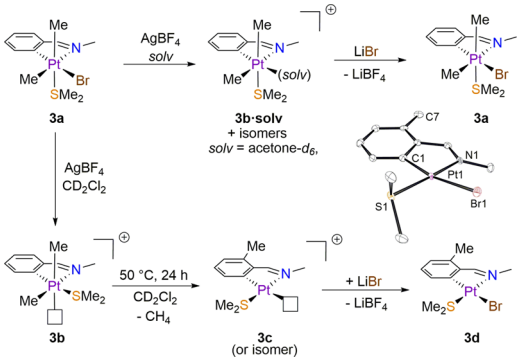

[a]Thermal ellipsoids shown at the 50% probability level.

Heating a solution of **3b** in CD_2Cl_2 at 50 °C for 24 h results in RE to form a single Pt^{II} product, **3c**, concomitant with the release of CH_4. In CD_2Cl_2 as well as more strongly coordinating solvents, **3c** exhibits broad signals, suggesting fluxional behavior, and LiBr was added to generate neutral **3d** to aid in characterization. Similar to what was observed for **1c·CH_3CN**, the HC═N ^{1}H NMR signal (δ = 8.43 ppm) exhibits large ^{195}Pt coupling (J_{PtH} = 124 Hz). The *trans*-relationship between N and SMe_2 was confirmed by a NOESY experiment, and a signal for the aryl-CH_3 group formed via Csp^2-Csp^3 coupling is present at 2.48 ppm. X-ray analysis of crystals of **3d** grown from a pentane solution provide a solid-state structure (Scheme 7) that is consistent with solution-state data.

Both **1b** and **3b** have Csp^3-Csp^3 and Csp^2-Csp^3 RE pathways accessible from low-energy isomers. To understand the unusual reactivity of **1b**, RE energy profiles were calculated for both species using DFT. From **1b**, Csp^3-Csp^3 reductive coupling to form a σ-ethane complex **1Int1** (ΔG = −8.4 kcal/mol) has an associated barrier of $\Delta G^{\ddagger}$ = 21.8 kcal/mol (Figure 1). Coupling of the Csp^2-Csp^3 groups to form **1Int2** was found to be an endergonic process (ΔG = 7.4 kcal/mol) and had an activation barrier that was higher by 2.4 kcal/mol, accounting for the selectivity observed experimentally.

For **3b**, a number of different RE pathways are available as a result of isomerization. The lowest-energy pathways were found

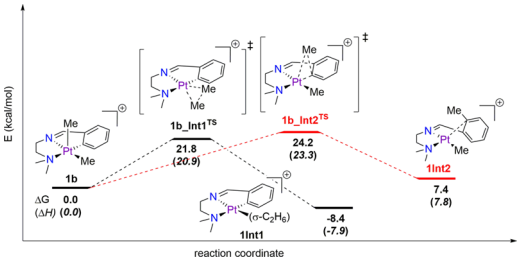

Figure 1. Calculated energy profile for reductive elimination from **1b** (Csp^3-Csp^3 in black, Csp^2-Csp^3 in red).

DOI: 10.1021/jacs.5b10993
J. Am. Chem. Soc. 2015, 137, 16004−16007

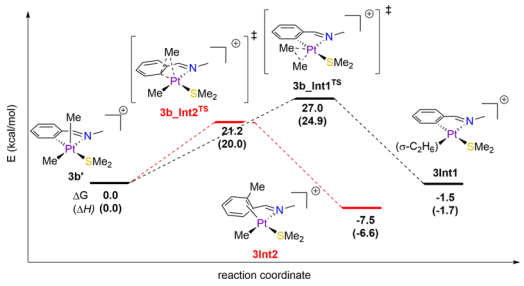

Figure 2. Calculated energy profile for reductive elimination from **3b′** (Csp^3-Csp^3 in black, Csp^2-Csp^3 in red).

to proceed directly from the square-pyramidal isomer of **3b′**, with SMe_2 *trans* to the aryl group (Figure 2).[12] Reductive coupling of Csp^2-Csp^3 groups from **3b′** proceeds though transition state **3b_Int2^{TS}** ($\Delta G^{\ddagger}$ = 21.2 kcal/mol) to form η^2-arene complex **3Int2**. Identification of the Csp^3-Csp^3 coupling pathway (**3b′**→**3b_Int1^{TS}**→**3Int1**) revealed that the barrier for C-C bond formation is 5.8 kcal/mol *higher* than the barrier for Csp^2-Csp^3 coupling, consistent with experimental observations.

A detailed examination of Csp^2-Csp^3 RE from **1b** and **3b** reveals significant differences between the systems. From **1b**, the reaction is endergonic, with a correspondingly late transition state with a C_{aryl}-Me bond distance of 1.89 Å (vs 1.95 Å in **3b_Int2^{TS}**). Despite the limited mobility of the arene ring in **3b**, NBO and orbital directionality analysis indicate that both systems proceed though the same concerted RE process (vs a 1,2-methyl shift).[12] The product **1Int2** of Csp^2-Csp^3 RE from **1b** can be described as an η^1-arene complex; although it is structurally similar to arenium complexes reported by van Koten et al.,[13] the small ring charge (q_{Ar} = +0.11e) and low Mayer bond order of the Pt-C_{ipso} bond (0.31) disfavor this assignment. As reductive coupling proceeds though the same intimate mechanism for both complexes, it appears that destabilization of the Pt^{II} arene product is responsible for the kinetic selectivity observed. This hypothesis is supported by comparison of **1Int1** with a calculated structure, **4Int1**,[12] with the ethylene linker broken and the arene ring free to adopt an ideal binding geometry. NBO analysis reveals that the arene in **4Int1** adopts an η^2 binding mode with an interaction energy 34 kcal/mol greater than that in **1Int1**. The Pt-N_{imine}-C_{aryl} angle is much smaller (95° vs 117°) and the N-Pt-N angle (104°) is larger than the bite angle in **1Int1** (82°), indicating that ligand flexibility is key in providing stability to Csp^2-Csp^3 RE products.

In conclusion, we report the first example of exclusive control over Csp^2-Csp^3 vs Csp^3-Csp^3 reductive elimination from a Pt^{IV} center bearing both Csp^2- and Csp^3-hybrizided hydrocarbyl groups, shown to be the result of kinetic selectivity by DFT calculations. We have demonstrated that selectivity in C-C RE from high-valent Pt^{IV} centers is governed not only by the hybridization of its hydrocarbyl substituents but also by the geometry and flexibility of the ligand scaffold.

■ ASSOCIATED CONTENT

Supporting Information

The Supporting Information is available free of charge on the ACS Publications website at DOI: 10.1021/jacs.5b10993.

Full computational and experimental details (PDF)

X-ray crystallographic data for **2d** and **3d** (CIF)

■ AUTHOR INFORMATION

Corresponding Author

*jenlove@chem.ubc.ca

Author Contributions

†E.G.B. and S.P. contributed equally.

Notes

The authors declare no competing financial interest.

■ ACKNOWLEDGMENTS

Acknowledgment is made to the donors of the American Chemical Society Petroleum Research Fund for partial support of this research (ACS PRF no. 53316-ND3). This research was enabled in part by the University of British Columbia, NSERC (Discovery and Research Tools and Instrumentation grants), the Canada Foundation for Innovation, WestGrid, and Compute Canada Calcul Canada. E.G.B. is grateful to NSERC for a CGS-M and to the Government of Canada for a Vanier Canada graduate scholarship. The authors thank Marcus W. Drover for help with X-ray crystallography and Addison N. Desnoyer for helpful discussions, as well as Weiling Chiu and Grete Hoffmann for assistance in ligand synthesis.

■ REFERENCES

(1) (a) Periana, R. A.; Taube, D. J.; Gamble, S.; Taube, H.; Satoh, T.; Fujii, H. *Science* **1998**, *280*, 560. (b) Lanci, M. P.; Remy, M. S.; Lao, D. B.; Sanford, M. S.; Mayer, J. M. *Organometallics* **2011**, *30*, 3704. (c) Caballero, A.; Pérez, P. J. *Chem. Soc. Rev.* **2013**, *42*, 8809.

(2) (a) Lersch, M.; Tilset, M. *Chem. Rev.* **2005**, *105*, 2471. (b) Shilov, A. E.; Shul'pin, G. B. *Activation and Catalytic Reactions of Saturated Hydrocarbons in the Presence of Metal Complexes*; Catalysis by Metal Complexes *21*; Springer: Berlin, 2000.

(3) (a) Wang, T.; Alfonso, B. J.; Love, J. A. *Org. Lett.* **2007**, *9*, 5629. (b) Wang, T.; Love, J. A. *Organometallics* **2008**, *27*, 3290. (c) Wang, T.; Keyes, L.; Patrick, B. O.; Love, J. A. *Organometallics* **2012**, *31*, 1397.

(4) Anderson, C. M.; Puddephatt, R. J.; Ferguson, G.; Lough, A. J. *J. Chem. Soc., Chem. Commun.* **1989**, 1297.

(5) (a) Crumpton, D. M.; Goldberg, K. I. *J. Am. Chem. Soc.* **2000**, *122*, 962. (b) Luedtke, A. T.; Goldberg, K. I. *Inorg. Chem.* **2007**, *46*, 8496. (c) Goldberg, K. I.; Yan, J. Y.; Winter, E. L. *J. Am. Chem. Soc.* **1994**, *116*, 1573. (d) Goldberg, K. I.; Yan, J. Y.; Breitung, E. M. *J. Am. Chem. Soc.* **1995**, *117*, 6889.

(6) Harkins, S. B.; Peters, J. C. *Organometallics* **2002**, *21*, 1753.

(7) (a) Maitlis, P. M.; Long, H. C.; Quyoum, R.; Turner, M. L.; Wang, Z.-Q. *Chem. Commun.* **1996**, 1. (b) Ananikov, V. P.; Musaev, D. G.; Morokuma, K. *Organometallics* **2005**, *24*, 715. (c) Ananikov, V. P.; Musaev, D. G.; Morokuma, K. *Eur. J. Inorg. Chem.* **2007**, *2007*, 5390.

(8) (a) Madison, B. L.; Thyme, S. B.; Keene, S.; Williams, B. S. *J. Am. Chem. Soc.* **2007**, *129*, 9538. (b) Jawad, J. K.; Puddephatt, R. J.; Stalteri, M. A. *Inorg. Chem.* **1982**, *21*, 332. (c) Gatard, S.; Çelenligil- Çetin, R.; Guo, C.; Foxman, B. M.; Ozerov, O. V. *J. Am. Chem. Soc.* **2006**, *128*, 2808. (d) Ghosh, R.; Emge, T. J.; Krogh-Jespersen, K.; Goldman, A. S. *J. Am. Chem. Soc.* **2008**, *130*, 11317.

(9) (a) Escolà, A.; Crespo, M.; Quirante, J.; Cortés, R.; Jayaraman, A.; Badía, J.; Baldomà, L.; Calvet, T.; Font-Bardía, M.; Cascante, M. *Organometallics* **2014**, *33*, 1740. (b) Anderson, C. M.; Crespo, M.; Jennings, M. C.; Lough, A. J.; Ferguson, G.; Puddephatt, R. J. *Organometallics* **1991**, *10*, 2672.

(10) Crespo, M.; Anderson, C. M.; Kfoury, N.; Font-Bardia, M.; Calvet, T. *Organometallics* **2012**, *31*, 4401.

(11) Crespo, M. *Polyhedron* **1996**, *15*, 1981.

(12) BP86/6-31G(d,p) level of theory; LANL2DZ + polarization for Pt, Br, S; solvation modeled using PCM. See SI for details.

(13) Albrecht, M.; Spek, A. L.; van Koten, G. *J. Am. Chem. Soc.* **2001**, *123*, 7233.

DOI: 10.1021/jacs.5b10993
J. Am. Chem. Soc. 2015, 137, 16004−16007